

# Superconducting Condensate Formation in Quasi-2D Systems with Arbitrary Carrier Density

Vadim M. Loktev<sup>1</sup>, Rachel M. Quick<sup>2\*</sup> and Sergei G. Sharapov<sup>2†</sup>

<sup>1</sup>*Bogolyubov Institute for Theoretical Physics, 252143 Kiev, Ukraine*

<sup>2</sup>*Department of Physics, University of Pretoria, 0002 Pretoria, South Africa*

(October 29, 1998)

A phase diagram for a quasi-2D metal with variable carrier density has been derived. The phases present are the normal phase, where the order parameter is zero; the pseudogap phase where the absolute value of the order parameter is non-zero but its phase is random, and a superconducting phase with a crossover quasi-2D Berezinskii-Kosterlitz-Thouless (BKT) region. The crossover region is bounded by the quasi-2D BKT temperature and the temperature for the onset of conventional long-range order (CLRO). The practical observation of these regions however critically depends on the carrier density. At high densities both the pseudogap and BKT regions vanish asymptotically i.e. one obtains the standard BCS picture. At intermediate densities the pseudogap phase is large but the BKT region negligible. Finally at very low densities both the pseudogap and BKT regions are sizeable. An attempt is made to explain the behaviour observed in underdoped (intermediate densities) and optimally doped high- $T_c$  superconducting compounds above their critical temperature. The transition to the pseudogap phase should also be regarded as a crossover.

74.72.-h, 74.20.Fg, 74.20.Mn, 64.60.Cn

*Key words:* quasi-2D metal, normal phase, pseudogap phase, superconducting phase

## I. INTRODUCTION

It is widely accepted [1–6] that the formation of the superconducting state in high-temperature superconductors (HTSCs) is quite different from traditional superconductors. The strongly anisotropic, almost two-dimensional, structure of HTSCs compounds increases significantly the influence of fluctuations and the different types of order appear to be separated on different energy scales. One type of order may correspond to the formation of a *pseudogap* (or lowered density of the states at the Fermi level) above the critical temperature  $T_c$  of the superconducting transition. The anomalous behaviour of HTSCs [3,7] (including the behaviour of the spin suscep-

tibility, resistivity, specific heat and photo-emission spectra) can then be interpreted in terms of the formation of this pseudogap [5,6,8].

There are many approaches for studying these extremely complicated systems. In most models, whether they are discrete (Hubbard) or continuous, the systems are treated as two dimensional (2D). Even the simplest 2D model with local nonretarded attraction between carriers is still a very rich and complicated system. Its properties beyond the mean field level are not well established, especially if one interested in a wide range of carrier densities and coupling strengths.

Most theoretical approaches (see, for example, [9,10] and the references therein) use the so called self-consistent T-matrix approximation, where all Green functions are "dressed". Although the self-consistency is an important feature [10–14], we stress that even this approximation cannot adequately describe the formation of the Berezinskii-Kosterlitz-Thouless (BKT) phase and it is well known that this is the only type of order possible in 2D [15]. The features of the superconducting BKT transition were studied in [16] although without self-consistency.

It is important to note, however, that often real systems (in particular HTSCs) are not strictly 2D systems and a pure 2D scenario cannot be applied to them directly. The presence of a third spatial direction already permits the formation of a superconducting phase with long-range order (LRO). One cannot say *a priori* that the formation of this phase destroys the 2D physics abruptly. Nevertheless, using some estimations obtained more than 20 years ago [17,18] for the quasi-1D metals, in principle even for relatively modest anisotropies and carrier densities the standard BCS behaviour should be recovered. The low and intermediate density limit is not as clear and, given the relevance of this limit to HTSCs with their small and variable carrier density, it should be examined carefully.

The purpose of this paper is to build the complete phase diagram of a quasi-2D metallic system with an arbitrary carrier density. We have considered both the conventional long-range order (CLRO) superconducting transition and the BKT transition. The accompanying publications were devoted to the calculation of the temperature for the BKT transition in the quasi-2D system [19], the temperature of the CLRO transition in the extreme Bose limit [20] (see also review [6]). To explain the origin of the whole phase diagram and especially the

\*Corresponding author, e-mail: rcarter@scientia.up.ac.za

†On leave of absence from Bogolyubov Institute for Theoretical Physics, 252143 Kiev, Ukraine

part related to the pseudogap region we recap here only the essential details from our previous works. The calculation for the temperature of the CLRO transition in the high density limit is new and we present here its full derivation (see also a preprint of authors devoted to the Coleman-Weinberg formalism in the theory of superconductivity [21]).

Indeed a quasi-2D BKT transition is only physically meaningful in the limit of weak three dimensionalization i.e. for a practically two dimensional system. In this limit we argue that for all carrier densities the BKT transition occurs before or at the CLRO phase. Certainly in the cuprates, there was until very recently little or no evidence for two superconducting phases and indeed it could be argued from experiment that there was only one superconducting transition. However in a recent paper [22] one indeed sees experimental evidence in underdoped Bicu-prates for the onset of planar superconductivity before that of superconductivity perpendicular to the planes. This experiment which gives a temperature difference of the order of 10K thus supports the picture of the formation of a quasi-2D BKT region prior to the formation of CLRO.

We also want to argue that the calculation of the critical temperatures for the quasi-2D BKT phase and the CLRO phase is very different both physically and mathematically. The BKT crossover region has a 2D counterpart since in two dimensions  $T_{\text{BKT}}$  is finite; the CLRO phase does not since  $T_c$  is zero [15]. Moreover at very low (physically unimportant) densities the transition temperatures are straightforward to calculate and very different [20]. The closeness of the two temperatures in the physically important region (close to optimal doping) is a non-trivial result since the calculations are different in both the physical assumptions made and the mathematical details of the approximations. We find it remarkable, given the highly anisotropic nature of the system, that the transition to conventional LRO takes place at a temperature close to that of the BKT transition.

We speculate that the quasi-2D BKT region corresponds to the crossover scale to three dimensional order. There may well be no sharp transition at the critical temperature for BKT phase formation.

More importantly, the superconducting region is separated from the normal phase by the pseudogap phase with nonzero neutral order parameter [16,19]. Clearly the transition to this phase should be a crossover but our approximations are insufficiently accurate to give this behaviour (see also discussion in [19]). Furthermore this phase is two dimensional and large enough to explain the observed anomalies when the density of the carriers is relatively low (the underdoped case). Nonetheless the transition to the superconducting phase is almost directly into a state with the conventional three-dimensional long-range order at relevant doping levels. Thus we have a crossover with increasing temperature from three dimensional behaviour in the superconducting state to two dimensional behaviour in the pseudogap phase similar to

the picture recently proposed by [23].

The rest of the paper is organized as follows. In Sec. II we introduce the model and sketch the formalism applied. This formalism is suitable for studying both the BKT and CLRO transitions. The equations for  $T_{\text{BKT}}^q$ , the temperature for the BKT transition in the quasi-2D system, have been derived previously [19] and are simply sketched. The CLRO superconducting transition temperature for small and relatively large carrier densities is derived in Sec. III. In the high density limit we go beyond the Nozières and Schmitt-Rink approach [24] which in the quasi-2D case, i.e. in the presence of a third direction, simply gives the BCS critical temperature. By employing the Coleman-Weinberg effective potential [25] we are able to calculate the Gaussian corrections to the critical temperature and we obtain the correct limiting behaviour  $T_c \rightarrow 0$  as the system becomes increasingly two-dimensional. The full phase diagram of the system is discussed in Sec. IV and Sec. V presents our conclusions.

## II. MODEL AND FORMALISM

Since the precise nature of the interplane tunneling in HTSCs is not yet known [26] several different models exist. Here we choose the simplest possible Hamiltonian density which is widely used in the study of HTSCs [27,20],

$$H = -\psi_\sigma^\dagger(\mathbf{r}) \left[ \frac{\nabla_\perp^2}{2m_\perp} + \frac{1}{m_z d^2} \cos(id\nabla_z) + \mu \right] \psi_\sigma(\mathbf{r}) - V \psi_\uparrow^\dagger(\mathbf{r}) \psi_\downarrow^\dagger(\mathbf{r}) \psi_\downarrow(\mathbf{r}) \psi_\uparrow(\mathbf{r}), \quad (2.1)$$

where  $\mathbf{r} \equiv \mathbf{r}_\perp, r_z$  (with  $\mathbf{r}_\perp$  being a 2D vector);  $\psi_\sigma(\mathbf{r})$  is a fermion field,  $\sigma = \uparrow, \downarrow$  is the spin variable;  $m_\perp$  is the effective carrier mass in the planes (for example  $\text{CuO}_2$  planes);  $m_z$  is an effective mass in the  $z$ -direction;  $d$  is the interlayer distance;  $V$  is an effective local attraction constant;  $\mu$  is a chemical potential which fixes the carrier density  $n_f$ ; and we take  $\hbar = k_B = 1$  and  $m_z \gg m_\perp$ .

In the weak coupling limit it is appropriate to replace the attraction constant  $V$  by the two-particle bound state energy in vacuum [28,29],

$$\varepsilon_b = -2W \exp\left(-\frac{4\pi d}{m_\perp V}\right). \quad (2.2)$$

Here  $W$  is the width in the plane and the limit  $V \rightarrow 0$ ,  $W \rightarrow \infty$  is to be understood. This replacement enables one to regularize the ultraviolet divergences in the theory. One can then define the dimensionless system parameter

$$\tilde{\epsilon} = \frac{\epsilon_F}{|\varepsilon_b|} \quad (2.3)$$

where  $\tilde{\epsilon} \ll 1$  corresponds to Bose or local pair superconductivity and  $\tilde{\epsilon} \gg 1$  to BCS superconductivity. Since

we have a quasi-2D system with a quadratic dispersion law in the planes the Fermi energy  $\epsilon_F$  is given by

$$\epsilon_F = \frac{\pi n_F d}{m_\perp}. \quad (2.4)$$

It was suggested in [30] that optimally doped HTSCs have  $\tilde{\epsilon} \sim 3 \cdot 10^2 - 10^3$  while conventional metallic superconductors have at least  $\tilde{\epsilon} \sim 10^3 - 10^4$ .

The proposed Hamiltonian proves very convenient for the study of fluctuation stabilization by weak 3D one-particle inter-plane tunneling. The two particle (Josephson) tunneling has been omitted in (2.1) on the assumption that it is less important than the one-particle coherent tunneling already included. In certain situations however Josephson tunneling is more important. In fact some authors consider the most important mechanism for HTSCs to be the incoherent inter-plane hopping (through, for instance, the impurity (localized) states or due to the assistance of phonons). Nonetheless we omit Josephson tunnelling here. However the single-particle dispersion relationship used here automatically incorporates the layered structure of HTSCs which is a vital extension to the commonly used 2D models.

It is significant that the large anisotropy in the conductivity cannot be related to the anisotropy in the effective masses  $m_z$  and  $m_\perp$ . In particular, HTSCs with rather large anisotropy in the  $z$ -direction do not display conventional metallic behaviour at low temperatures [31]. However this semiconducting behaviour is not directly related to the pseudogap phenomena [31] and the Hamiltonian (2.1) may be used to study the qualitative features of pseudogap opening.

The standard Hubbard-Stratonovich method was used to study the Hamiltonian (2.1). In this method the statistical sum  $Z(v, \mu, T)$  ( $v$  is the volume of the system) is formally rewritten as a functional integral over the auxiliary fields  $\Phi = V\psi_\downarrow\psi_\uparrow$  and  $\Phi^* = V\psi_\uparrow^\dagger\psi_\downarrow^\dagger$

$$Z(v, \mu, T) = \int \mathcal{D}\Phi \mathcal{D}\Phi^* \exp[-\beta\Omega(v, \mu, T, \Phi(x), \Phi^*(x))], \quad (2.5)$$

where

$$\beta\Omega(v, \mu, T, \Phi(x), \Phi^*(x)) = \frac{1}{V} \int_0^\beta d\tau \int d\mathbf{r} |\Phi(x)|^2 - \text{Tr} \text{Ln} G^{-1}[\Phi(x), \Phi^*(x)] \quad (2.6)$$

is the effective action and  $x = \tau, \mathbf{r}$  denotes both the imaginary time  $\tau$  and the position  $\mathbf{r}$  previously defined. The action (2.6) is expressed in terms of the Green function  $G$  which has the following operator form

$$G^{-1}[\Phi(x), \Phi^*(x)] = -\hat{I}\partial_\tau + \tau_3 \left[ \frac{\nabla_\perp^2}{2m_\perp} + \frac{1}{m_z d^2} \cos(id\nabla_z) + \mu \right] + \tau_+ \Phi(x) + \tau_- \Phi^*(x). \quad (2.7)$$

where  $\tau_3, \tau_\pm = (\tau_1 \pm i\tau_2)/2$  are Pauli matrices. Although the representation (2.5), (2.6) is exact, in practical calculations it is necessary to restrict ourselves to some approximation. The most convenient approximation for our purposes is the Coleman-Weinberg [25] (see also [32]) effective potential in the one-loop approximation which we will use for studying LRO. The exact expression (2.5) is replaced by

$$Z(v, \mu, T, |\Phi|^2) = \exp[-\beta\Omega_{pot}(v, \mu, T, |\Phi|^2)], \quad (2.8)$$

where the effective thermodynamical potential

$$\Omega_{pot}(v, \mu, T, |\Phi|^2) \simeq \Omega_{pot}^{MF}(v, \mu, T, |\Phi|^2) + \Omega^{(1)}(v, \mu, T, |\Phi|^2) \quad (2.9)$$

is expressed through the mean-field "tree-potential"

$$\Omega_{pot}^{MF}(v, \mu, T, |\Phi|^2) = \Omega(v, \mu, T, \Phi(x), \Phi^*(x))|_{\Phi, \Phi^* = \text{const}} \quad (2.10)$$

and the one-loop (quantum) correction

$$\Omega^{(1)}(v, \mu, T, |\Phi|^2) = \frac{T}{2} \text{Tr} \text{Ln} \Gamma_+^{-1} + \frac{T}{2} \text{Tr} \text{Ln} \Gamma_-^{-1} \quad (2.11)$$

Here the Green functions  $\Gamma_\pm$  are given by

$$\begin{aligned} \Gamma_\pm^{-1}(\tau, \mathbf{r}) &= \left[ \frac{\beta\delta^2\Omega}{\delta\Phi^*(\tau, \mathbf{r})\delta\Phi(0, 0)} \pm \frac{\beta\delta^2\Omega}{\delta\Phi^*(\tau, \mathbf{r})\delta\Phi^*(0, 0)} \right]_{\Phi=\Phi^* = |\Phi| = \text{const}} \\ &= \frac{1}{V} \delta(\tau)\delta(\mathbf{r}) + \text{tr}[G(\tau, \mathbf{r})\tau_+ G(-\tau, -\mathbf{r})\tau_-] \\ &\pm \text{tr}[G(\tau, \mathbf{r})\tau_- G(-\tau, -\mathbf{r})\tau_+]. \end{aligned} \quad (2.12)$$

Strictly speaking one can only use this factorization into  $\Gamma_+^{-1}\Gamma_-^{-1}$  in the limit of small momenta and frequencies and high carrier density [33]. While the representation (2.5), (2.6) is convenient for the studying of the LRO transition, the formation of the BKT and pseudogap phases demands a more subtle treatment. This is related to the fact that these phases do not display LRO. This is evident in the original 2D model [16] where LRO is forbidden by the 2D theorems [15].

Thus one must avoid the presupposition about the existence of LRO used to write down the expression (2.9). The illegal step in the treatment based on representation (2.5), (2.6) is the fixing of a definite value to the phase  $\theta$  of the complex order parameter  $\Phi$  which is performed when one obtains Eq. (2.9). To avoid this dangerous step one must use the modulus,  $\rho(x)$ , and phase,  $\theta(x)$ , parameterization of the order parameter  $\Phi(x) = \rho(x) \exp[i\theta(x)]$  as first pointed out by Witten [34]. This particular choice of parameterisation ensures that  $\Phi(x)$  is single-valued with period  $2\pi$ . At the same time as this replacement by modulus-phase variables, one must reparameterize the Nambu spinor as  $\psi_\sigma(x) = \chi_\sigma(x) \exp[i\theta(x)/2]$ .

As a result we have obtained [19] instead of (2.5), (2.6) the following representation

$$Z(v, \mu, T) = \int \rho \mathcal{D}\rho \mathcal{D}\theta \exp[-\beta \Omega(v, \mu, T, \rho(x), \partial\theta(x))], \quad (2.13)$$

where the one-loop effective action  $\Omega(v, \mu, T, \rho(x), \partial\theta(x))$  now depends on the modulus-phase variables and has been evaluated in [19] where we have shown that

$$\Omega \simeq \Omega_{kin}(v, \mu, T, \rho, \partial\theta) + \Omega_{pot}^{MF}(v, \mu, T, \rho) \quad (2.14)$$

where the potential energy term in terms of  $\rho^2$  is identical to the mean-field potential in the BCS approximation but with  $|\Phi|^2$  replaced by  $\rho^2$ . Thus  $T_\rho$ , the temperature at which  $\rho = 0$ , is in this approximation identical to the BCS mean field temperature  $T_c^{MF}$ . However, although  $T_\rho = T_c^{MF}$  in the mean-field approximation for  $\rho(x)$ , the two temperatures have a very different basis, both mathematically and physically [16,19].

It has been shown that, in the model under consideration, the kinetic energy term reduces in lowest order to [19] the Hamiltonian for the classical spin quasi-2D XY model [35] (see also [36,37]) and we have simply used their expression for the BKT transition in the highly anisotropic case, when the vortex ring excitations are irrelevant [35].

A self-consistent calculation of  $T_{BKT}^q$  as a function of  $n_f$  also requires additional equations for  $\rho$  and  $\mu$ . The relevant equations are given by minimizing the potential  $\Omega_{pot}$  with respect to  $\rho$  and fixing the number density.

The numerical investigation of  $T_{BKT}^q$  and  $T_\rho$  has been carried out (see [19]) and fortunately gives results not too different from the 2D case [16].

### III. SUPERCONDUCTING TRANSITION INTO THE PHASE WITH LONG-RANGE ORDER

As discussed in Section II to study CLRO formation one should use the effective potential (2.9) obtained in the Gaussian approximation.

There are two limiting cases where one can obtain an analytical solution, namely, the low and high density limits. For small concentrations of the carriers we have previously obtained the critical temperature [20] using the approach developed by Nozières and Schmitt-Rink [24] (see also [38,39]), while for the high density case we employ a new method similar to that used in [37].

The main point of [24] is the solution of the system of number and gap equations derived using the potential (2.9) but with the one-loop corrections (2.11) taken on the critical line  $\Phi = \Phi^* = 0$ . This means that the effect of the fluctuations is only included through the number equation, while the gap equation is derived using the mean field potential. Thus one always recovers the standard mean-field (BCS) gap equation

$$\frac{1}{V} = \int \frac{d\mathbf{k}}{(2\pi)^3} \frac{1}{2\xi(\mathbf{k})} \tanh \frac{\xi(\mathbf{k})}{2T_c}, \quad (3.1)$$

where  $\xi(\mathbf{k}) = k_\perp^2/2m - (m_z d^2)^{-1} \cos k_z d - \mu$ , while the corresponding number equation has the form

$$n_F(\mu, T_c) + 2n_B(\mu, T_c) = n_f. \quad (3.2)$$

One can see from (3.2) that the fermions are divided into two coexisting systems: fermi-particles, or unbound fermions with density  $n_F(\mu, T_c)$ , and local pairs, or bosons with density  $n_B(\mu, T_c)$ . In the extreme Bose limit  $n_F = 0$  the temperature has already been shown to be the Bose condensation temperature of an ideal quasi-2D Bose-gas [20,40]

We now consider the high-density limit. This case is characterized by the condition that the Fermi surface is not disturbed by the attractive interaction, i.e. the contribution of the bosons to (3.2) is negligible and  $\mu \simeq \epsilon_F$ . Thus one need only study the gap equation. It is evident that the Nozières and Schmitt-Rink approach which yields the mean-field equation (3.1) cannot describe a quasi-2D system adequately. Indeed it follows from the 2D theorems that in the limit  $m_z \rightarrow \infty$ , when the system becomes two dimensional, the value of  $T_c$  must go to zero. Clearly this can never be obtained from Eq. (3.1).

To obtain the gap equation which does describe the quasi-2D system one must include the fluctuations. This can be done if uses the effective potential (2.9) with the one-loop correction (2.11) but without setting  $\Phi = \Phi^* = 0$  prior to taking the derivative with respect to  $\Phi$ .

Thus the gap equation takes the form

$$\left. \frac{\partial \Omega_{pot}^{MF}(v, \mu, T_c, |\Phi|^2)}{\partial |\Phi|^2} \right|_{\Phi=\Phi^*=0} + \left. \frac{\partial \Omega^{(1)}(v, \mu, T_c, |\Phi|^2)}{\partial |\Phi|^2} \right|_{\Phi=\Phi^*=0} = 0 \quad (3.3)$$

where the quantum correction (2.11) which was omitted in (3.1) has now been included.

There is a subtle point related to Eq.(3.3). The value of  $T_c$  defined by Eq.(3.3) should be less then the mean-field temperature,  $T_c^{MF}$  defined by Eq.(3.1) (and given by (A.11)) in the high-density limit  $\mu = \epsilon_F \gg T_c^{MF}$ . However sketching the tree-potential  $\Omega_{pot}^{MF}(T)$  as a function of  $\Phi$  for  $T < T_c^{MF}$  yields the Mexican hat shape. This has a minimum at  $|\Phi|^2 = \Phi_{min}^2 \neq 0$  (where  $\Phi_{min}$  is simply the mean-field value for  $\Phi$ ) but a maximum at  $\Phi = \Phi^* = 0$ . Thus the role of the correction to the effective potential in Eq.(3.3) is to transform the maximum of the tree-potential to a minimum of the full potential  $\Omega_{pot}(|\Phi|^2)$ .

Unfortunately, the one-loop correction  $\Omega^{(1)}$  defined by (2.11) is ill-defined (complex) at the point of interest. The temperature at which the potential just becomes complex in fact gives the Thouless criteria of superconductivity in BCS theory. However, in our treatment this

is only an indication that the one-loop approximation fails at the point  $\Phi = \Phi^* = 0$  and is evidently related to the non-convexity of  $\Omega_{pot}^{MF}(|\Phi|^2)$  at this point.

This situation is standard in quantum field theory if one considers the class of theories with tree-level symmetry breaking and an extensive literature exists [32,41–43]. In our case to describe a homogeneous state where  $|\Phi|^2$  is uniform one should replace  $\Omega_{pot}$  by the so called Gaussian [41] or modified [42] effective potential which coincides with  $\Omega_{pot}$  in the region where the latter is well-defined.

One could now find the modified potential, but we will use here, in our opinion, a more transparent consideration which will allow us to evaluate the one-loop correction not at  $\Phi = 0$  but in the region where it is well-defined and coincides with the modified potential. Our results can then be straightforwardly related to the modified potential of Weinberg [42].

Let us assume that  $T_c \lesssim T_c^{MF}$  which means the point  $\Phi_{min}$  is close to zero. At this point  $\Omega_{pot}^{MF}$  is surely convex and the one-loop correction (2.11) is real and well-defined. Thus for  $T_c \lesssim T_c^{MF}$  one can approximate Eq.(3.3) by

$$\frac{1}{v} \frac{\partial \Omega_{pot}^{MF}(v, \epsilon_F, T_c, \Phi^2)}{\partial \Phi^2} \Big|_{\Phi=0} + \frac{1}{v} \frac{\partial \Omega^{(1)}(v, \epsilon_F, T_c, \Phi^2)}{\partial \Phi^2} \Big|_{\Phi=\Phi_{min}} = 0, \quad (3.4)$$

where we choose  $\Phi$  to be real and the value of  $\Phi_{min}$  is simply the well-known mean-field BCS value for  $\Phi$  at temperature  $T$  (see e.g. [44] and Appendix A Eq. (A.13)).

Therefore to solve the approximated gap equation (3.4) one has to calculate

$$\frac{1}{v} \frac{\partial \Omega^{(1)}(v, \epsilon_F, T, \Phi^2)}{\partial \Phi^2} \Big|_{\Phi=\Phi_{min}} = \frac{1}{2} \frac{T}{(2\pi)^3} \sum_{\pm} \sum_{n=-\infty}^{\infty} \int d\mathbf{K} \Gamma_{\pm}(i\Omega_n, \mathbf{K}) \frac{\partial \Gamma_{\pm}^{-1}(i\Omega_n, \mathbf{K})}{\partial \Phi^2} \Big|_{\Phi=\Phi_{min}}, \quad (3.5)$$

where  $\mathbf{K} = (\mathbf{K}_{\perp}, K_z)$  and, starting from (2.12), one can obtain the Green's functions as a function of  $\Phi$  in the momentum representation

$$\Gamma_{\pm}^{-1}(i\Omega_n, \mathbf{K}) = \frac{1}{V} + \frac{T}{(2\pi)^3} \sum_{l=-\infty}^{\infty} \int d\mathbf{k} \times \frac{[i\omega_l - \xi_{\pm}][i\omega_l + i\Omega_n + \xi_{\pm}] \pm \Phi^2}{[\omega_l^2 + \xi_{\pm}^2 + \Phi^2][(\omega_l + \Omega_n)^2 + \xi_{\pm}^2 + \Phi^2]}, \quad (3.6)$$

where we have introduced the short-hand notation  $\xi_{\pm} = \xi(\mathbf{k} \pm \mathbf{K}/2)$  and  $\Omega_n = 2\pi nT$ ,  $\omega_l = \pi(2l+1)T$  are odd and even Matsubara frequencies, respectively.

Since  $\Gamma^{-1}(0, \mathbf{0}) = 0$  is simply the BCS gap equation it has solution  $\Phi$  equal to the BCS value  $\Phi_{min}$  i.e. for  $\Phi = \Phi_{min}$ ,  $\Gamma^{-1}(0, \mathbf{K})$  has a zero at  $\mathbf{K} = 0$ . This gives rise to the only singular term in (3.5) for  $\Phi = \Phi_{min}$ , namely the pole in  $\Gamma_{-}(0, \mathbf{K})$  at  $\mathbf{K} = 0$ . One can therefore write

$$\frac{1}{v} \frac{\partial \Omega^{(1)}(v, \epsilon_F, T, \Phi^2)}{\partial \Phi^2} \Big|_{\Phi=\Phi_{min}} \simeq \frac{1}{2} \frac{T}{(2\pi)^3} \int d\mathbf{K} \Gamma_{-}(0, \mathbf{K}) \Big|_{\Phi=\Phi_{min}} \frac{\partial \Gamma_{-}^{-1}(0, \mathbf{K})}{\partial \Phi^2} \Big|_{\Phi=\Phi_{min}} \quad (3.7)$$

In order to perform the calculations analytically we use the derivative expansion for the Green function  $\Gamma_{-}^{-1}$ ,

$$\Gamma_{-}^{-1}(0, \mathbf{K}) \Big|_{\Phi=\Phi_{min}} = \frac{m_{\perp}}{2\pi d} [a\mathbf{K}_{\perp}^2 + b[1 - \cos K_z d]], \quad (3.8)$$

(see Appendix A, Eqs.(A.10) and (A.12)) and its derivative

$$\frac{\partial \Gamma_{-}^{-1}(0, \mathbf{K})}{\partial \Phi^2} \Big|_{\Phi=\Phi_{min}} = \frac{m_{\perp} c}{2\pi d} \quad (3.9)$$

(see Appendix A, Eqs. (A.3) and (A.4)).

Substituting these two expressions into (3.7), one arrives at the following approximation

$$\frac{1}{v} \frac{\partial \Omega^{(1)}(v, \epsilon_F, T, \Phi^2)}{\partial \Phi^2} \Big|_{\Phi=\Phi_{min}} \simeq \frac{1}{2} \frac{T}{(2\pi)^3} \int d\mathbf{K} \frac{c}{a\mathbf{K}_{\perp}^2 + b[1 - \cos K_z d]}. \quad (3.10)$$

One can see that Eq.(3.10) has no infrared divergencies due to the presence of the third direction ( $b \neq 0$ ). In two dimensions it would be infrared divergent as required by the 2D theorems [15]. This equation also has an artificial ultraviolet divergence as a result of the replacement of the Green's function  $\Gamma^{-1}$  by its derivative approximation. Thus one should introduce a rather natural ultraviolet cutoff  $(\mathbf{K}_{\perp}^{max})^2 = 2m_{\perp}\Phi(T=0) = 2m_{\perp}\sqrt{2|\epsilon_b|\epsilon_F}$  and integrate over the momentum  $\mathbf{K}$  to obtain the expression

$$\frac{1}{v} \frac{\partial \Omega^{(1)}(v, \epsilon_F, T, \Phi^2)}{\partial \Phi^2} \Big|_{\Phi=\Phi_{min}} \simeq \frac{m_{\perp}}{2\pi d} \frac{T}{2\epsilon_F} |\ln \kappa|, \quad (3.11)$$

where

$$\kappa = \frac{1}{4\sqrt{2}} \frac{w^2}{\epsilon_F^2} \sqrt{\frac{\epsilon_F}{|\epsilon_b|}}, \quad w = \frac{1}{m_z d^2}. \quad (3.12)$$

Substituting (3.11) into (3.4) one obtains the final transcendental equation for  $T_c$

$$\ln \frac{T_c}{T_c^{MF}} + \frac{T_c}{2\epsilon_F} |\ln \kappa| = 0, \quad (3.13)$$

which may be rewritten in the following more convenient form

$$T_c = 2\epsilon_F \frac{|\ln(T_c/T_c^{MF})|}{|\ln \kappa|}. \quad (3.14)$$

Strictly speaking the equation (3.14) is only valid when  $T_c \lesssim T_c^{MF}$ . However, we intend to use Eq.(3.14) even

when  $T_c < T_c^{MF}$ , which will allow to qualitatively sketch the whole phase diagram of the system.

If one solves (3.14) numerically for reasonable width one obtains roughly linear behaviour  $T_c \sim \epsilon_F \sim n_f$  for a wide range of intermediate densities (see below). This dependence is observed experimentally [4] for HTSCs samples which have a Fermi surface.

A second feature of (3.14) is that increasing  $|\epsilon_b|$  increases both  $T_c^{MF}$  and  $T_c$ . This is opposite to the behaviour in the low density limit. Finally  $T_c$  goes to zero as  $m_z \rightarrow \infty$  ( $w \rightarrow 0$ ) as it must. This is very different to the limiting behaviour of  $T_{\text{BKT}}^q$ , namely  $T_{\text{BKT}}^q \rightarrow T_{\text{BKT}}$  in the limit  $m_z \rightarrow \infty$ .

As stated above one can also understand the approximation used in (3.4) in terms of the modified effective potential defined in [42]. The modified effective potential in [42] is defined as the minimum value for  $\Omega$  given a homogeneous state where  $|\Phi|^2$  is uniform. The real part of this modified potential has the following form

$$\tilde{\Omega}^{(1)}(v, \mu, T, |\Phi|^2) = \frac{T}{2(2\pi)^3} \sum_{\pm} \sum_{n=-\infty}^{\infty} \int_{\mathcal{D}} d\mathbf{K} \ln \Gamma_{\pm}^{-1}(i\Omega_n, \mathbf{K}), \quad (3.15)$$

where the area  $\mathcal{D}$  of integration in the momentum space includes only positive modes. One can see that (3.15) indeed coincides with (2.11) when  $\Omega^{(1)}$  is well-defined. Furthermore the modified potential (3.15) leads to the gap equation (3.4) which was considered above as the approximated one.

In the region  $\Phi < \Phi_{min}$  the modified effective potential considered above differs from the traditional effective potential,  $\Omega_{eff}(\Phi)$ , which is defined as the minimum value for  $\Omega$  such that the space average of  $\Phi(x)$  is given by  $\Phi$ . It can be shown that the conventional effective potential is in fact the convex envelope of the modified effective potential and is real and convex everywhere. However for  $\Phi < \Phi_{min}$  it describes an inhomogeneous mixed state where the value of  $\Phi(x)$  is not uniform in space. One can readily understand that the modified and not the original potential is relevant for the superconducting state.

There is, however, the difference between our interpretation of the modified potential and that of [42]. In [42] the homogeneous state described by (3.15) is considered as decaying and the rate of the decay is related to negative modes of (2.11) which are not included in (3.15). It is physically obvious that there is no real decay of the homogeneous superconducting state with  $\Phi < \Phi_{min}$  for  $T < T_c$  although we have not been able to prove this rigorously. The absence of decay is in agreement with the interpretation of [41] although it should be stressed that the modified potential discussed here is not identical to the Gaussian effective potential in [41].

#### IV. THE PHASE DIAGRAM OF THE SYSTEM

We have now obtained solutions for  $T_c$ ,  $T_{\text{BKT}}^q$  and  $T_\rho$  and can build the phase diagram for the quasi-2D system. This diagram comprises the normal phase, the pseudogap phase, the superconducting BKT region, and the CLRO phase with superconductivity in the bulk in order of decreasing temperature. The practical observation of these regions (i.e. the temperature range for which they are present) is however critically dependent on the carrier density.

*i)* We first reiterate results at very low carrier densities  $\tilde{\epsilon} \ll 1$  i.e. for a Bose liquid of isolated local pairs.

Firstly, the critical temperature is linear in  $\epsilon_F$   $T_c \sim \epsilon_F$  (or  $T_c \sim n_f$  as expected in the 2D case) [20]. For large anisotropy the proportionality constant depends only on the particle density and the width in the z-direction. This constant is less than 1/8 for half-bandwidth

$$w \leq \frac{\sqrt{2|\epsilon_b|\epsilon_F}}{2\sqrt{2}\exp 2} = \frac{\Phi(T=0)}{2\sqrt{2}\exp 2} \quad (4.1)$$

where  $\Phi(T=0)$  is the zero-temperature energy gap. Recall that in the 3D case  $T_c \sim n_f^{2/3}$  [38]. Secondly, contrary to the case of a 3D superconductor where  $T_c$  is independent of  $V$  [38], in a quasi-2D system  $T_c$  does depend on  $V$ . In particular  $T_c$  decreases with the growth of  $V$ . The reason for this is the dynamical increasing of the composite boson mass in the third direction. Thus, the growth of  $|\epsilon_b|$  (or equivalently of  $V$ ) "makes" the system more and more two-dimensional in this model of a quasi-2D metal with a local four-fermion interaction. It is interesting to note that a decreasing  $T_c$  can also take place in the case when the local pairs are bipolarons [45].

Furthermore the temperature  $T_{\text{BKT}}^q$  always lies above  $T_c$  in this limit for reasonable bandwidths (see Eq. (4.1) and strongly anisotropic systems [16,19] since

$$T_{\text{BKT}}^q > T_{\text{BKT}} = \frac{\epsilon_F}{8}. \quad (4.2)$$

In addition the BKT region and LRO order phase are of roughly equal size so one expects to see an extensive region where the interlayer tunneling is insufficient to produce CLRO.

This range of carrier densities is not however experimentally important because the anomalous behaviour of HTSCs is observed when the Fermi surface is still present.

*ii)* We next present results for high carrier densities ( $\tilde{\epsilon} \gg 10^3$ ).

At high carrier densities  $T_c$  approaches  $T_c^{MF}$  asymptotically so that the condition  $T_c \lesssim T_c^{MF}$  is satisfied and equation (3.14) for the critical temperature is indeed valid. Furthermore one can expand the logarithm in equation (3.14) to give

$$T_c = T_\rho \left( 1 - \frac{T_\rho |\ln \kappa|}{2\epsilon_F} \right), \quad \tilde{\epsilon} \gtrsim 10^3 \quad (4.3)$$

where  $T_c^{MF}$  has been replaced by the temperature  $T_\rho$  (which is identical in the approximation used in this paper).

For these carrier densities one also finds that  $\rho(T_{\text{BKT}})/T_{\text{BKT}} \ll 1$  which yields the following estimation for the BKT transition temperature

$$T_\rho > T_{\text{BKT}}^q > T_{\text{BKT}} \simeq T_\rho \left(1 - \frac{4T_\rho}{\epsilon_F}\right), \quad \tilde{\epsilon} \gtrsim 10^3. \quad (4.4)$$

From (4.3) and (4.4) it follows that  $T_{\text{BKT}}^q \geq T_c$  for reasonable anisotropies, bandwidths satisfying (4.1) and for particle density,  $\tilde{\epsilon} > 1/2(e/2)^8$  which is clearly satisfied in the high-density region. Furthermore both  $T_c$  and  $T_{\text{BKT}}^q$  tend asymptotically to  $T_\rho = T_c^{MF}$  in the high density limit. Thus both the pseudogap and BKT regions vanish asymptotically in this limit and one recovers the standard BCS behaviour with a transition directly into a superconducting state with CLRO at the BCS critical temperature as obtained by [17] in the quasi-1D case and in the weak-coupling limit in 2D [5,16,46].

*iii)* The physical interest lies at intermediate densities ( $\tilde{\epsilon} \sim 10 - 10^3$ ). Optimal doping corresponds to  $\tilde{\epsilon} \sim 3 \cdot 10^2 - 10^3$  [30] and we show this range of densities in Fig. 1. The precise value of  $\tilde{\epsilon}$  for optimal doping is however strongly dependent on the anisotropy of the system. For these relatively high densities the condition  $T_{\text{BKT}}^q, T_c \lesssim T_c^{MF}$  is still satisfied and equation (3.14) is a good approximation. For example, for  $\tilde{\epsilon} = 700$ ,  $(T_\rho - T_c)/T_c \approx 0.15$ , indicating that both the pseudogap and BKT regions are small. One can see from Eq. (4.3) that

$$\frac{T_\rho - T_c}{T_c} \rightarrow 0, \quad \tilde{\epsilon} \rightarrow \infty \quad (4.5)$$

This gives an asymptotic disappearance of the pseudogap since the fraction of the temperature range in the pseudogap phase goes to zero. This corresponds to the experimental observations. Furthermore one finds that  $T_c$  is very close to  $T_{\text{BKT}}^q$  which is in agreement with the experimental observation of at most a very narrow crossover region in temperature from two-dimensional to three-dimensional superconductivity reported in [47,22] for optimally doped cuprates.

Due to the fact that the Fermi surface is still present for the densities where the pseudogap develops, one might expect the pseudogap phenomena to occur at  $\tilde{\epsilon} \sim 10 - 10^2$ . Extrapolating (3.14) to these densities one finds that  $T_c$  is always less than  $T_{\text{BKT}}^q$ . More essentially  $(T_\rho - T_{\text{BKT}}^q)/T_\rho \sim 1$ , i.e. the pseudogap phase is big enough to make it observed and sufficient to explain the observed anomalies in the underdoped compounds. On the other hand  $(T_{\text{BKT}}^q - T_c)/T_c \ll 1$  so that the BKT region again remains relatively small. In this density range these two temperatures are so close that one cannot see the difference on the phase diagram. The phase diagram is thus unchanged from that shown in [19] since the lines for  $T_c$  and  $T_{\text{BKT}}^q$  coincide. Thus for all carrier densities

appropriate to HTSCs the superconducting transition is practically directly to the phase with CLRO. Since the temperature range for the BKT region is only a few degrees it has until recently [22] lain within the observed critical region.

We note that our results for  $T_c$  imply that the quasi-2D BKT region is decreasing in size with decreasing density. We believe that this is not the case physically particularly since it has been shown that in the Bose limit the quasi-2D BKT region is large. Thus we believe that this is an artifact of our approximation since it becomes less accurate as  $T_c$  moves away from  $T_\rho$  which occurs with decreasing density (see discussion after Eq. (3.14)). Thus, although one can say that this transitional temperature range is small, our approximation is not adequate to describe its dependence on the carrier density.

## V. CONCLUDING REMARKS

We have derived a phase diagram for a superconducting quasi-2D system in which one has four regions. These are the normal phase, the pseudogap region, the BKT region and the phase with conventional bulk superconductivity (CLRO).

For all realistic carrier densities we find the BKT region to be only a few degrees. This implies that it lies within the critical region and is difficult to observe experimentally. In fact  $T_{\text{BKT}}^q$  is slightly overestimated (since for example the effect of vortex rings is omitted). In contrast the value of  $T_c$  is underestimated by the approximation used since only one loop corrections have been included [37]. Thus the BKT region, if present, is even smaller than calculated.

In contrast the pseudogap region is substantial for the underdoped region where the unusual superconducting condensate formation is responsible for the observed anomalies in underdoped HTSCs. At optimal doping the pseudogap phase is also negligible and one recovers the standard BCS behaviour.

With the calculation of  $T_c$  we are able to present a picture in which two dimensional behaviour predominates in the pseudogap phase but where the superconducting phase is three dimensional in line with the recent result of [23].

## ACKNOWLEDGMENTS

We gratefully acknowledge E.V. Gorbary and V.P. Gusynin for proofreading the manuscript and valuable suggestions. We also thank N.J. Davidson, V.A. Miransky, I.A. Shovkovy and O. Tchernyshyov for fruitful discussions. One of us (S.G.Sh) is grateful to the members of the Department of Physics of the University of Pretoria for hospitality. R.M.Q and S.G.Sh acknowl-

edge the financial support of the Foundation for Research Development, Pretoria.

## APPENDIX A: THE CALCULATION OF THE GREEN FUNCTIONS $\Gamma_{\pm}$

We derive here the Green functions  $\Gamma_{\pm}(i\Omega_n, \mathbf{K})$  in the derivative approximation for the large density ( $\mu \simeq \epsilon_F \gg T$ ) limit starting from expression (3.6). Since  $\Phi/T \ll 1$  for  $T \lesssim T_c$  one can use the "high-temperature" approximation

$$\frac{1}{\omega_n^2 + \xi^2 + \Phi^2} \simeq \frac{1}{\omega_n^2 + \xi^2} - \frac{\Phi^2}{[\omega_n^2 + \xi^2]^2}, \quad (\text{A.1})$$

which gives

$$\Gamma_{\pm}^{-1}(i\Omega_n, \mathbf{K}) = \frac{1}{V} + T \sum_{l=-\infty}^{\infty} \int \frac{d\mathbf{k}}{(2\pi)^3} \times \left\{ \frac{1}{[i\omega_l + \xi_-][i\omega_l + i\Omega_n - \xi_+]} + \frac{2\Phi^2 \pm \Phi^2}{[\omega_l^2 + \xi^2]^2} \right\}. \quad (\text{A.2})$$

where to lowest order one can set  $\Omega_n = \mathbf{K} = 0$  in the  $\Phi^2$  term. Performing the summation over fermion Matsubara frequencies one arrives at the following result

$$\Gamma_{\pm}^{-1}(i\Omega_n, \mathbf{K}) = \Gamma^{-1}(i\Omega_n, \mathbf{K}) + \frac{m_{\perp}}{2\pi d} c(2\Phi^2 \pm \Phi^2), \quad (\text{A.3})$$

where in for large densities

$$c = \frac{7\zeta(3)}{8\pi^2 T^2} \quad (\text{A.4})$$

and  $\Gamma(i\Omega_n, \mathbf{K})$  is the Green function of the order parameter fluctuations in the normal ( $\Phi, \Phi^* = 0$ ) state:

$$\Gamma^{-1}(i\Omega_n, \mathbf{K}) = \frac{1}{V} - \frac{1}{2} \int \frac{d\mathbf{k}}{(2\pi)^3} \frac{1}{\xi_+ + \xi_- - i\Omega_n} \times \left[ \tanh \frac{\xi_+}{2T} + \tanh \frac{\xi_-}{2T} \right]. \quad (\text{A.5})$$

The 2D limit ( $w = 0$ ) of the Green function was studied by Shovkovy et al. [48,49] and we need to generalize the expression to the quasi-2D case. Substituting the coupling constant  $V$  expressed via the bound state energy (2.2) into (A.5) and performing simple transformations on the hyperbolic functions one arrives at

$$\begin{aligned} \Gamma^{-1}(i\Omega_n, \mathbf{K}) &= \frac{m_{\perp}}{4\pi d} \ln \frac{2W}{|\epsilon_b|} \\ &- \frac{m_{\perp}}{8\pi^2 d} \int_0^{2W} dx \int_0^{2\pi} dt \frac{1}{x + s(t, K_{\perp}, K_z) - i\Omega_n} \\ &\times \tanh \frac{x + s(t, K_{\perp}, K_z)}{4T} \\ &+ \frac{m_{\perp}}{8\pi^2 d} \int_0^{2W} dx \int_0^{2\pi} dt \frac{2}{\pi} \int_0^{\pi/2} d\varphi \frac{1}{x + s(t, K_{\perp}, K_z) - i\Omega_n} \end{aligned}$$

$$\begin{aligned} &\times \tanh \frac{x + s(t, K_{\perp}, K_z)}{4T} \times \\ &\frac{\cosh \frac{d(t, K_{\perp}, K_z, \cos \varphi)}{2T} - 1}{\cosh \frac{x + s(t, K_{\perp}, K_z)}{2T} + \cosh \frac{d(t, K_{\perp}, K_z, \cos \varphi)}{2T}}, \quad (\text{A.6}) \end{aligned}$$

where we introduced the short-hand notations

$$s(t, K_{\perp}, K_z) = \frac{K_{\perp}^2}{4m_{\perp}} - 2w \cos t \cos \left( \frac{K_z d}{2} \right) - 2\mu$$

and

$$d(t, K_{\perp}, K_z, \cos \varphi) = \frac{k_{\perp} K_{\perp} \cos \varphi}{m_{\perp}} + 2w \sin t \sin \left( \frac{K_z d}{2} \right).$$

Using the identities:

$$\begin{aligned} \frac{1}{x + s(t, K_{\perp}, K_z) - i\Omega_n} &= \frac{1}{x + s(t, K_{\perp}, K_z)} \\ &+ \frac{i\Omega_n}{[x + s(t, K_{\perp}, K_z)][x + s(t, K_{\perp}, K_z) - i\Omega_n]}, \quad (\text{A.7}) \end{aligned}$$

and

$$\int_0^a \frac{dx}{x} \tanh x = \ln \frac{4a\gamma}{\pi} - \int_a^{\infty} \frac{dx}{x} (\tanh x - 1), \quad \text{at } a > 0, \quad (\text{A.8})$$

( $\ln \gamma$  is the Euler constant), one can take the limit  $W \rightarrow \infty$  in (A.6) and come to the expression:

$$\begin{aligned} \Gamma^{-1}(i\Omega_n, \mathbf{K}) &= \frac{m_{\perp}}{4\pi d} \ln \frac{\pi T}{|\epsilon_b| \gamma} \\ &+ \frac{m_{\perp}}{8\pi^2 d} \int_0^{2\pi} dt \int_0^1 \frac{dx}{x} \tanh \left[ x \frac{s(t, K_{\perp}, K_z)}{4T} \right] \\ &- i\Omega_n \frac{m_{\perp}}{8\pi^2 d} \int_0^{2\pi} dt \int_0^{\infty} dx \\ &\frac{1}{[x + s(t, K_{\perp}, K_z)][x + s(t, K_{\perp}, K_z) - i\Omega_n]} \\ &\times \tanh \frac{x + s(t, K_{\perp}, K_z)}{4T} \\ &+ \frac{m_{\perp}}{8\pi^2 d} \int_0^{2\pi} dt \int_0^{\infty} dx \frac{1}{\pi} \int_0^{\pi} d\varphi \frac{1}{x + s(t, K_{\perp}, K_z) - i\Omega_n} \\ &\times \tanh \frac{x + s(t, K_{\perp}, K_z)}{4T} \times \\ &\frac{\cosh \frac{d(t, K_{\perp}, K_z, \cos \varphi)}{2T} - 1}{\cosh \frac{x + s(t, K_{\perp}, K_z)}{2T} + \cosh \frac{d(t, K_{\perp}, K_z, \cos \varphi)}{2T}}. \quad (\text{A.9}) \end{aligned}$$

One may easily show that in the 2D limit  $w \rightarrow 0$  the expression (A.9) transforms into the Green function obtained in [48]. For example, the last term of (A.9) gives the exact representation for the imaginary part of this function.



We, however, are interested in the derivative expansion of  $\Gamma^{-1}(0, \mathbf{K})$  for the anisotropies  $w/T \ll 1$  and large densities which has the following form

$$\Gamma^{-1}(0, \mathbf{K}) = \frac{m_{\perp}}{2\pi d} \left[ \ln \left( \frac{T}{T_c^{MF}} \right) + aK_{\perp}^2 + b[1 - \cos K_z d] \right], \quad (\text{A.10})$$

where

$$T_c^{MF} = \frac{\gamma}{\pi} \sqrt{2|\varepsilon_b|\epsilon_F} \quad (\text{A.11})$$

is the mean-field transition temperature obtained from the mean-field gap equation (3.1);

$$a = \frac{7\zeta(3)}{(4\pi)^2} \frac{\epsilon_F}{m_{\perp} T^2}, \quad b = \frac{7\zeta(3)}{(4\pi)^2} \frac{w^2}{T^2}. \quad (\text{A.12})$$

Again the expression (A.10) is in the correspondence with the Green function used in [49]. We note also that the anisotropy  $\alpha(\epsilon_F) = bd^2/2a$  is equal to the anisotropy that was found in the quasi-2D BKT model [19].

Finally we should stress that if one substitutes into (A.3) (see also (A.10)) the well-known mean-field BCS dependence (see e.g. [44])

$$\Phi_{min}^2(T) = \frac{8\pi^2(T_c^{MF})^2}{7\zeta(3)} \left( 1 - \frac{T}{T_c^{MF}} \right) \quad (\text{A.13})$$

of the gap on the temperature near  $T_c^{MF}$ , one obtains (3.8) which shows that  $\Gamma_{+}(0, \mathbf{K}) > 0$ , while  $\Gamma_{-}(0, \mathbf{K}) \leq 0$  with the pole at  $\mathbf{K} = 0$ .

---

[1] M. Randeria, in *Bose Einstein Condensation*, edited by A. Griffin, D.W. Snoke, and S. Stringari (Cambridge U.P. New York, 1995) p.355.  
[2] V. Emery, S.A. Kivelson, *Nature* 374 (1995) 434; *Phys. Rev. Lett.* 74 (1995) 3253.  
[3] V.M. Loktev, *Fiz. Nizk. Temp.* 22 (1996) 3 [Engl. Trans.: *Low Temp. Phys.* 22 (1996) 1].  
[4] Y.J. Uemura, Preprint cond-mat/9706151, *Physica C* 282 (1997) 194.  
[5] M. Randeria, *Varenna Lectures*, Preprint cond-mat/9710223.  
[6] V.M. Loktev and S.G. Sharapov, *Cond. Mat. Phys. (Lviv)* 11 (1997) 131 (Preprint cond-mat/9706285).  
[7] D. Pines, *Tr.J. of Physics*, 20 (1996) 535.  
[8] H. Ding, T. Yokoya, I.C. Campuzano et al., *Nature* 382 (1996) 51.  
[9] R. Micnas, M.H. Pedersen, S. Schafroth et al., *Phys. Rev. B* 52 (1995) 16223.  
[10] O. Tchernyshyov, *Phys. Rev. B* 56 (1997) 3372.  
[11] J.O. Sofo, C.A. Balseiro, *Phys. Rev. B* 45 (1992) 8197.  
[12] J.W. Serene, *Phys. Rev. B* 40 (1989) 10873; J.W. Serene and D.W. Hess, *Phys. Rev. B* 44 (1991) 3391.

[13] B. Janko, J. Maly, K. Levin, *Phys. Rev. B* 56 (1997) R11407.  
[14] J.R. Engelbrecht, A. Nazarenko, M. Randeria and E. Dagotto, *Phys. Rev. B* 57 (1998) 13406.  
[15] N.D. Mermim, H. Wagner, *Phys. Rev. Lett.* 17 (1966) 1113; P.C. Hohenberg, *Phys. Rev.* 158 (1967) 383; S. Coleman, *Comm. Math. Phys.* 31 (1973) 259.  
[16] V.P. Gusynin, V.M. Loktev, S.G. Sharapov, *Pis'ma Zh. Eksp. Teor. Phys.* 65 (1997) 170 [Engl. Trans.: *JETP Lett.* 65 (1997) 182]; *Fiz. Nizk. Temp.* 23 (1997) 816 [Engl. Trans.: *Low Temp. Phys.* 23 (1997) 612]; Preprint cond-mat/9709034, accepted for publication in *JETP*.  
[17] I.E. Dzyaloshinskii, E.I. Kats, *Zh. Eksp. Teor. Phys.* 55 (1968) 2373.  
[18] K.B. Efetov, A.I. Larkin, *Zh. Eksp. Teor. Phys.* 66 (1974) 2290 [Engl. Trans.: *JETP* 39 (1974) 1129];  
[19] R.M. Quick, S.G. Sharapov, *Physica C* 301 (1998) 262.  
[20] E.V. Gorbar, V.M. Loktev, S.G. Sharapov, *Physica C* 257 (1996) 355.  
[21] R.M. Quick, S.G. Sharapov, Preprint cond-mat/9804310.  
[22] V.N. Zverev, D.V. Shovkun, I.G. Naumenko, *Pis'ma Zh. Eksp. Teor. Phys.* 68 (1998) 309 [Engl. Trans.: *JETP Lett.* (1998)].  
[23] G. Preosti, Y. M. Vilks, M. R. Norman, Preprint cond-mat/9808298.  
[24] P. Nozières and S. Schmitt-Rink, *J. Low Temp. Phys.* 59 (1985) 195.  
[25] S. Coleman, E. Weinberg, *Phys. Rev. D* 7 (1973) 1888.  
[26] J. Shützman *et al.*, *Phys. Rev. B* 55 (1997) 11118.  
[27] M.R. Cimberle *et al.*, *Phys. Rev. B* 55 (1997) 14745.  
[28] K. Miyake, *Prog. Theor. Phys.* 69 (1983) 1794.  
[29] E.V. Gorbar, V.P. Gusynin, V.M. Loktev, *Fiz. Nizk. Temp.* 19 (1993) 1171 [Engl. Trans.: *Low Temp. Phys.* 19 (1993) 832]; Preprint ITP-92-54E (1992).  
[30] M. Casas, J.M. Getino, M. de Llano *et al.*, *Phys. Rev. B* 50 (1994) 15945.  
[31] T. Watanabe, T. Fujii, A. Matsuda, *Phys. Rev. Lett.* 79 (1997) 2113.  
[32] V.A. Miransky, *Dynamical Symmetry Breaking in Quantum Field Theory*, (World Scientific Co., Singapore, 1993).  
[33] V.N. Popov, *Functional Integrals in Quantum Field Theory and Statistical Physics*, (Kluwer Academic Publishers, Dordrecht, Holland, 1983).  
[34] E. Witten, *Nucl. Phys. B* 145 (1978) 110.  
[35] S. Hikami, T. Tsuneto, *Prog. Theor. Phys.* 63 (1980) 387.  
[36] T.V. Ramakrishnan, *Physica Scripta T* 27 (1989) 24.  
[37] H. Yamamoto, I. Ichinose, *Nucl. Phys. B* 370 (1992) 695.  
[38] C.A.R. Sá de Melo, M. Randeria, and J.R. Engelbrecht, *Phys. Rev. Lett.* 71 (1993) 3202.  
[39] R. Haussmann, *Phys. Rev. B* 49 (1994) 12975.  
[40] X.-G. Wen and R. Kan, *Phys. Rev. B* 37 (1988) 595.  
[41] P.M. Stevenson, *Phys. Rev. D* 30 (1984) 1712; *ibid* 32 (1985) 1389.  
[42] E.J. Weinberg, A. Wu *Phys. Rev. D* 36 (1987) 2474.  
[43] M. Sher, *Phys. Rep.* 179 (1989) 273.  
[44] A. Fetter, D. Walecka, *Quantum theory of many-particle*

*systems*, (McGraw-Hill, New York, 1971).

- [45] A.S. Alexandrov and A.B. Krebs, Usp. Fiz. Nauk, 162, No. 5 (1992) 1.
- [46] E. Babaev, H. Kleinert, Preprint cond-mat/9804206.
- [47] P.C.E. Stamp, L. Forro and C. Ayache, Phys. Rev. B 38 (1988) 2847.
- [48] I.A. Shovkovy, private communication.
- [49] V.M. Loktev, S.G. Sharapov, Fiz. Nizk. Temp. 23 (1997) 180 [Engl. Trans.: Low Temp. Phys. 23 132 (1997) 132].

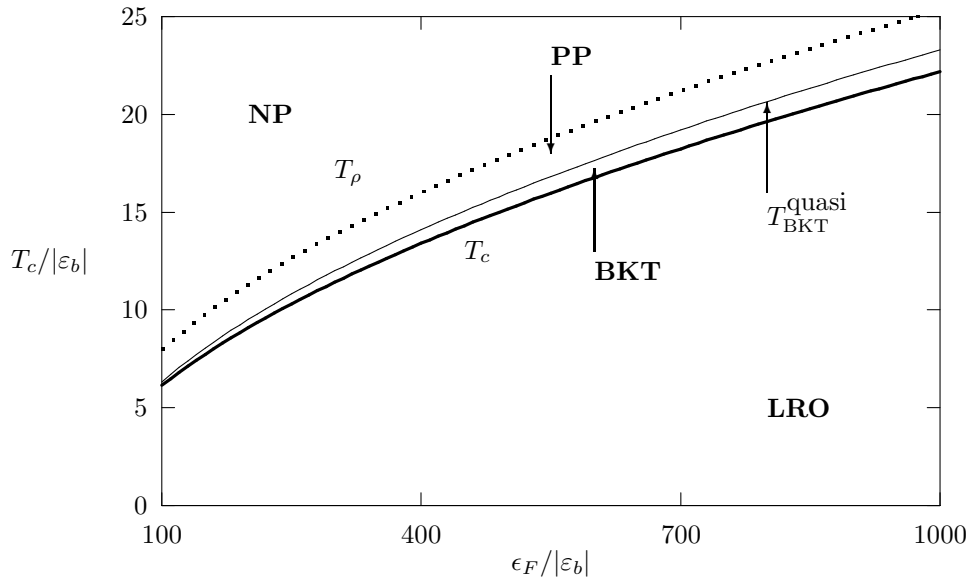


FIG. 1.  $T_c$ ,  $T_{\text{BKT}}^q$  and  $T_\rho = T_c^{MF}$  versus noninteracting fermion density. The regions of the normal phase (NP), pseudogap phase (PP), BKT phase and long-range order (LRO) phase are indicated. We assumed that  $m_z/m_\perp = 100$  and  $(m_z d^2 |\epsilon_b|)^{-1} = 1$ .